Towards the systematic reconnaissance of seismic signals from glaciers and ice sheets - Part A: Event detection for cryoseismology: Supplementary Materials

Rebecca B. Latto[1], Ross J. Turner[1], Anya M. Reading[1], and J. Paul Winberry[2]

[1]School of Natural Sciences (Physics), University of Tasmania, Private Bag 37, Hobart, 7001, Australia

[2]Department of Geological Sciences, Central Washington University, Ellensburg, WA, USA

Table of Contents

2) Electronic Supplements

Supplementary files for the implementation of the multi-STA/LTA algorithm are publicly available in https://github.com/beccalatto/multi_sta_lta/, including:

30   **MultiSTALTA_UseGuide.pdf** : How-to guide to download the multi-STA/LTA function and use in ObsPy

    entry_points.txt : Replacement text file for implementing multi-STA/LTA in Python

    trigger.py : ObsPy script with all native trigger routines and including the multi-STA/LTA routine

Supplementary files related to material presented in the main text are publicly available in https://github.com/beccalatto/multi_sta_lta/event_detection_for_cryoseismology/.

35   Repository architecture, including folder and file names with descriptions, is listed below.

a) Detection catalogues

    ReferenceEventCatalogueWhillans_MultiSTALTA.csv : Reference event catalogue for the Whillans Ice Stream from the multi-STA/LTA algorithm

    TraceEventCatalogueWhillans_MultiSTALTA.csv : Trace event catalogue for the Whillans Ice Stream from the multi-

40   STA/LTA algorithm

    ReferenceEventCatalogueWhillans_RECmin.csv : Reference event catalogue for the Whillans Ice Stream from the recursive algorithm with RECmin parameters

    TraceEventCatalogueWhillans_RECmin.csv : Trace event catalogue for the Whillans Ice Stream from the recursive algorithm with RECmin parameters

45   **ReferenceEventCatalogueWhillans_RECmax.csv** : Reference event catalogue for the Whillans Ice Stream from the recursive algorithm with RECmax parameters

    TraceEventCatalogueWhillans_RECmax.csv : Trace event catalogue for the Whillans Ice Stream from the recursive algorithm with RECmax parameters

b) Labelled catalogues

50   **ReferenceEventCatalogueWhillans_MultiSTALTA_ConfidenceAssignments.csv** : Reference event catalogue for the Whillans Ice Stream from the multi-STA/LTA algorithm with high and low confidence assignments

    ReferenceEventCatalogueWhillans_MultiSTALTA_KnownSeismicity.csv : Reference event catalogue for the Whillans Ice Stream from the multi-STA/LTA algorithm with identified stick-slip and teleseisms events

    ReferenceEventCatalogueWhillans_MultiSTALTA_TidesTable.txt : The .txt file contains all of the reference cata-

55   logue columns as well as tidal height per event, tidal height derivative (increasing or decreasing), absolute tidal height

behavior (more or less positive, more or less negative), and inflection type (minimum, maximum, or none). Tidal information results from the Circum-Antarctic Tidal Simulation for the location downstream from the grounding line of the Whillans Ice Stream (coordinate: 84°20'20.3994"S -166°0'0"W) (Padman et al., 2002; Howard, 2019)

c) Parameter evaluation

EventDetectSection2.ipynb : Open access Python notebook used for the computational analysis and compilation of figures. Notebook sections organized by:

☐ 2.2a Simulation of test waveforms for algorithm development

☐ 2.2a.1 Representative event classes

☐ 2.2a.2 Simulated seismic signal

☐ 2.2b Parameter search to optimize the application of the multi-STA/LTA

☐ 2.2b.1 Defining the fine-grid of parameters

☐ 2.2b.2 Assessing for probability of event detection

☐ 2.2b.3 Parameter search results

☐ 2.2b.5 Comparison of algorithms for synthetic data

d) MyAnalystPlots

MyAnalystPlots.py : Routine that plots events from the multi_sta_lta catalogue. The script enables for event viewing in all three components (E,N,Z) and all stations that detect an event.

MyAnalystREADME.txt : Use guide for MyAnalystPlots.py.

MyAnalystPlots produced PDFs of the waveform views of the known Whillans Ice Stream seismicity are made available separately at https://cloudstor.aarnet.edu.au/plus/s/sLD2R6miP2wXoLY. Each product is divided into sets capped at 20 slides. The filenames are as follows:

MyAnalystPlot_STICK-SLIP_PRATT14_set0–6.pdf
MyAnalystPlot_STICK-SLIP_PRATT14 ADDITIONAL.pdf
MyAnalystPlot_TELESEISM I_set0–1.pdf
MyAnalystPlot_TELESEISM II_set0–1.pdf

S2.2a Simulation of test waveforms for algorithm development

In Sect. 2.2 in the main text, we describe the Monte Carlo simulation that enabled algorithm testing and optimization for the multi-STA/LTA algorithm. In this supplement, we provide further discussion on applied methods.

85 #### S2.2a.1 Representative event classes

The two classes of simulated events both include a low-frequency oscillation in the signal with a frequency between 1 and 1/10th of the event duration. The amplitude of the signal is assumed to decay exponentially after the start of the event. The second class of event further includes a high-frequency component to the signal with a frequency of between 1/10 and 1/100th of the duration. The functional form of these two classes of event is given by:

90
$$\text{Event}\,1(t) = A\sin\left(\frac{2\pi nt}{T}\right) e^{-\beta t/T} \tag{S1a}$$

$$\text{Event}\,2(t) = A\sin\left(\frac{2\pi mt}{T}\right)\left(1 - \gamma\sin\left(\frac{2\pi nt}{T}\right)\right) e^{-\beta t/T}, \tag{S1b}$$

where A is the initial amplitude of the event, T is the duration of the event, n and m are the order of the low- and high-frequency components of the event respectively (i.e. $f_n = n/T$ and $f_m = m/T$), β is the decay rate (related to the attenuation constant as $\alpha = \beta/T$), and γ is a constant which controls the relative amplitude of the high- to low-frequency oscillations. The

95 values for each of these variables are randomly sampled for a uniform distribution in $\log_{10}$ space (main text, Table 2) to create a population of simulated events.

S2.2a.2 Simulated seismic signal

The seismic signal is created by combining events from our simulated population at random separations and adding random background noise. The background noise for a whole day (86400 seconds) is created by randomly sampling a normal dis-

100 tribution with mean zero and standard deviation of $\sigma = 1$ (the amplitude of our simulated events is thus equivalent to the signal-to-noise level).

We must include two events in the test waveforms to account for the case of a low frequency and low amplitude event immediately following a high amplitude event. The second event in this scenario requires long values of sta and lta to detect its low frequency signal, however, these will remain raised from the preceding high amplitude for an appreciable time. Pairs

105 of events are therefore an important test case that must be included in our simulated signals. We randomly choose the event class with equal likelihood; the first event is placed at a constant time of 10 hours and the second event a random time after the cessation of the first. The initial 10 hours of noise prior to the first event is determined as an adequate amount of time to establish a representative long term average of the noise. We provide example outputs of the constructed simulated signal that show how the two event classes manifest in a single day-long waveform (Fig. S1). It is not informative to include more than

110 two events in each simulated signal because the detection of events is largely independent of the properties of previous events.

We generate 100 random Monte Carlo realizations of the day-long seismic signal with simulated event durations, amplitudes, decay rates and frequency composition. This simulation size was chosen to provide sufficient sampling to yield a stable result for optimal parameter choices, within a practical time frame for computation.
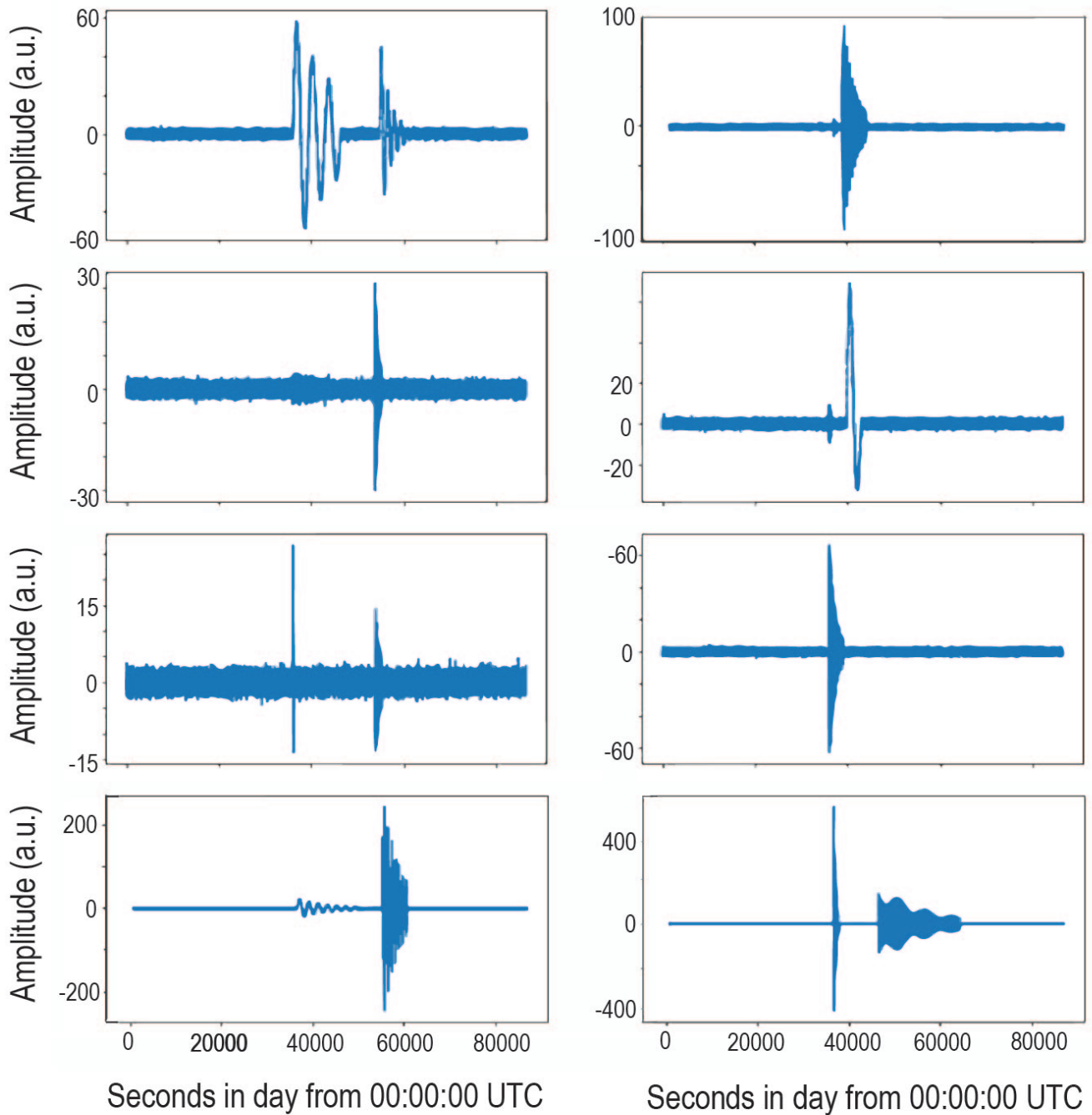
Figure S1. Example outputs of the constructed simulated signal. In the period of one day (86400 seconds), we show how the two pseudo-randomly picked and generated event classes manifest in a single day-long waveform outputs of the simulated signals. A Monte Carlo approach is used to provide a set of waveforms for algorithm development, as detailed in main text.

S2.2b Parameter search to optimize the application of the multi-STA/LTA

In this section, we refer to Figs. 2 and 3 from Sect. 2.2 in main text with elaborated discussion. To inform the choice of optimal parameters, we apply the multi-STA/LTA algorithm over a grid of such parameters to each simulated waveform generated as above. We maintain a trigger threshold value for the hybrid CF of 3, and a detrigger threshold of 1.

S2.2b.1 Defining the fine-grid of parameters

The five parameters in Eq. (1) are sampled over a fine grid of plausible values, uniformly distributed in log space (Table 1), excluding combinations of parameters that preferentially select random noise. Values of lta greater than 100 seconds paired with the higher Δ_{lta} values tested (factor of 1000) yield unrealistic results because the length of the day is 86400 seconds, therefore, we also exclude values of lta > 100 s. Values of Δ_{sta} or Δ_{lta} = 1 are equivalent to the recursive STA/LTA so those values are also excluded from testing noting that we compare the new algorithm to the recursive STA/LTA algorithm later in this section. We choose the minimum value of each of these parameters to be 10. When analyzing results, we require that the smallest lta is greater than the largest sta. The sta also has to be greater than one over the Nyquist frequency to eliminate aliasing (Oppenheim et al., 2001; Barruol et al., 2013). The Nyquist frequency is defined as one-half of the sampling rate. Here, the Nyquist frequency is one-half of 200 Hz, i.e. 100 Hz. Therefore, our minimum sta is 0.01 seconds.

S2.2b.2 Assessing the success of event detection

In the analysis that follows, the null hypothesis is that a set of algorithm parameters yield no preference towards selecting the simulated events over the random noise (Cressie and Read, 1984). We quantify the success of parameters by using the probability measure, p-value. Lower p-values correspond to a stronger rejection of the null hypothesis, i.e. a higher chance that we are detecting events rather than random noise, however, lower p-values could also be the result of false positives, which means that the null hypothesis is incorrectly rejected. Typically, p-values less than 0.05 (a 5.0% chance of a false positive) are considered to be statistically significant, and in order to further decrease uncertainty we limit our focus to results with p-values less than 0.005 (i.e. a 0.5% chance of a false positive; Benjamin et al., 2018). The p-values are calculated by considering the percentage of a simulated event length that is detected as a single event. The total p-value informs which sets of parameters best detect both events in each simulated waveform as two single events. For our current purpose, this metric quantifies the ability to generate a catalogue of distinct, real events.

For each set of algorithm parameters, the p-values are combined using Fisher's method (Fisher, 1925). This produces a chi-squared statistic χ^2 for the given set of parameters applied over the sampled random variations in the simulated events:

$$\chi^2_{2k} \approx -2 \sum_{i=1}^{k} \ln(p_i), \tag{S2}$$

where $k = 100$ is the number of Monte Carlo realizations when the simulations are completely independent, and p_i is the p-value calculated for the ith realisation. The total p-value is calculated using a distribution with $2k$ degrees of freedom.

According to Brown's method, an extension of Fisher's, the degrees of freedom will be less than $2k$ when simulations have dependence (Brown, 1975). As we do not know the exact number of dependencies, we assume that the Monte Carlo waveform simulations have a high level of dependence and conservatively apply a degree of freedom of $k = 1$.

The marginal probability quantifies the probability of detection for a certain (marginal) parameter without considering the other parameters, and is calculated by summing the total probabilities over all algorithm parameters except the marginal parameter. For example, the marginal probability distribution for sta is found using

$$p_{\text{marginal}}(\text{sta}) = \sum_i \sum_j \sum_k \sum_l p_{\text{total}}(\text{sta}, \text{lta}_i, \Delta_{\text{sta},j}, \Delta_{\text{lta},k}, \epsilon_l). \tag{S3}$$

The two-dimensional marginal probability distribution is calculated by summing the total probabilities over all algorithm parameters except two marginal parameters, revealing the interaction between parameters. The conditional probability of detection for a parameter (or parameters) depends on the choice of another parameter (or parameters), and is particularly useful in this application because the probability of detecting an event is reliant on the combination of chosen parameters. A probability can be both marginal and conditional when only a marginal parameter is considered, based on the choice of (i.e. conditioned by) another parameter.

S2.2b.3 Parameter search results

We first look at the marginal distributions for each parameter (Fig. 2, blue circles). The marginal probabilities of lta, Δ_{sta}, Δ_{lta}, and ϵ do not yield significant results, as they are all above the indicated threshold. In contrast, there is a range of comparable p-values that are below the threshold for a given sta between 0.01 to 0.18, where the sta value that is at the absolute minimum p-value occurs at 0.03. We therefore condition the other parameters according to this sta range. Shown in Fig. 2 (green squares), lta is at a significant, absolute minimum p-value at 100. In this case, a successful detection at an lta of 100 is about 10^8 more certain than at an lta of 50. Though significant, the respective Δ_{sta} and Δ_{lta} p-values are higher than that of the minimum lta p-value by at least 10^4. This indicates that these p-values correspond to parameter values that yield less certainty for detection. The p-values for ϵ are not significant. Since we wish to ensure our set of parameters produce a self-consistent solution, we proceed by conditioning the probability using the previous sta range and lta of 100.

In Figure 2 (red triangles), we see the significant probabilities of Δ_{sta} and Δ_{lta} fall within a wide range. For Δ_{sta}, values 10–300 are significant and for Δ_{lta}, values 20–1000 are significant. Since these results are inconclusive, we present the two-dimensional marginal probability of these parameters in Fig. 3. The Δ_{sta}, Δ_{lta} pairs that yield the highest chance of successful event detection (i.e. lowest p-values) fall along a diagonal line: $log_{10}(\Delta_{\text{lta}}) = 1.24 \times log_{10}(\Delta_{\text{sta}}) + 0.06$ (shown in red on Fig. 3 to inform further analyses). The values for Δ_{sta} and Δ_{lta} can be chosen from parameter combinations along, or close to, a line of best fit. We note that Δ_{sta} of 18 and Δ_{lta} of 56 are at the local minima along the line of best fit in Fig. 3.

Finally, to determine ϵ, we condition the probability with the sta range between 0.01 and 0.18, lta at 100, and Δ_{sta} and Δ_{lta} along the line $log_{10}(\Delta_{\text{lta}}) = 1.24 \times log_{10}(\Delta_{\text{sta}}) + 0.06$ (Fig. 2; black diamonds). Accordingly, any ϵ between 10 and 100 results in the same success in event detection. To confirm, we compare p-values computed from the same sta range, lta of 100, and

Δ_{sta} and Δ_{lta} from the end points of the best fit line (equal to $\Delta_{\text{sta}} = 10$ and $\Delta_{\text{lta}} = 18$; $\Delta_{\text{sta}} = 178$ and $\Delta_{\text{lta}} = 1000$). We find that the p-value is consistently stable from ϵ of 10 to 100 for both Δ_{sta} and Δ_{lta} end points. By Eq. (1) with an lta of 100, an ϵ of 100 yields 2 sta, lta pairs and an ϵ of 10 yields 4 pairs. We exclude other significant values of ϵ because, below 10, random noise is more likely to get detected with the increased number of pairs.

S2.2b.4 Parameter recommendations

Recommended parameters for the optimized application of the multi-STA/LTA algorithm, from the above analysis, are therefore sta = 0.03 and lta = 100. While sta and lta are clear choices, the other parameters are less exact. Good parameter choices for Δ_{sta} and Δ_{lta} lie along the red line in Fig. 3 and between ϵ of 10 and 100 in Fig. 2 (black diamonds). We choose $\Delta_{\text{sta}} = 18$ and $\Delta_{\text{lta}} = 56$, as these values are the (gentle) local minima in probability in Fig. 3 and also cover a reasonable variety of sta, lta pairs. Since each of the pairs yield approximately equal probability, a choice of optimal values that falls anywhere along the indicated line is valid. With regard to ϵ, our goal is to detect diverse seismic signals from glaciers ranging from seconds to hours, so the set of sta, lta pairs employed should represent this spread. A lower ϵ guarantees more sta, lta pairs without compromising computing efficiency or probability of event detection, which supports our choice of $\epsilon = 10$.

The selected parameters (i.e. sta = 0.03 s, lta = 100 s, $\Delta_{\text{sta}} = 18$, $\Delta_{\text{lta}} = 56$, $\epsilon = 10$) will be referred to in later sections as the *recommended parameters* for implementation of the multi-STA/LTA algorithm. We further discuss parameter choice strategies in Sect. 4.1.

S2.2b.5 Comparison of algorithms for synthetic data

We repeat the process of assessing the probability of event detection detailed in Sect. 5 and Sect. 5, substituting the recursive STA/LTA algorithm for the multi-STA/LTA and then running event detection over the set of simulated waveforms. Our aim is to compare how each algorithm detects events with its own set of recommended parameters.

We recall that for the recursive STA/LTA algorithm, the equivalent left hand side of Eq. (1) has the form

$C_{\text{recursive}}(A_{\text{on}}, A_{\text{off}}, \text{sta}, \text{lta})$, where $C_{\text{recursive}}$ refers to the characteristic function of the recursive algorithm, A_{on} and A_{off} are thresholds for which an event is triggered and detriggered respectively, and sta and lta are user-determined parameter choices (there are no Δ_{sta}, Δ_{lta}, or ϵ parameters). Some equivalency between algorithms can be established as the multi-STA/LTA algorithm runs a certain number (defined by ϵ) of sta, lta pairs through the recursive STA/LTA algorithm. We note that even with the same sta, lta pair inputs, the recursive STA/LTA algorithm would differ from the multi-STA/LTA in that it computes CFs individually by sta, lta pair without any optimization. As such, we establish a set of sta, lta pairs that make the two algorithms comparable to a reasonable extent.

The p-value over 100 recursive STA/LTA simulated detections for sta = 0.03 s, lta = 100 s is 3×10^{-43}; the p-value for sta = 0.54 s, lta = 5600 s is 9×10^{-40} (Table S1). For the multi-STA/LTA simulated detections with optimized parameters, the p-value is 8×10^{-45}. In this comparison, the null hypothesis (that events and noise are just as likely to be detected) is rejected with a probability 10^2–10^5 times smaller for multi-STA/LTA on average. Essentially, the multi-STA/LTA algorithm yields more realistic events from event detection than the recursive algorithm, even with equivalent sta and lta values. We attribute

the improvement to the recursive algorithm running each of these pairs individually, while the multi-STA/LTA runs the pairs
210   collectively and outputs the event for the optimized CF.

Recursive	sta	lta				p-value
	0.03	100				3×10^{-43}
	0.54	5600				9×10^{-40}
multi-STA/LTA	sta	lta	Δ_{sta}	Δ_{lta}	ϵ	p-value
	0.03	100	18	56	10	8×10^{-45}

Table S1. Overview of comparison of algorithms results for synthetic data. The recursive parameter values for sta and lta (top section) chosen as equivalent to the multi-STA/LTA recommended parameters (bottom section) and the computed p-value per parameter set over the 100 Monte Carlo waveform simulations. Users can follow along the methodology for comparison with the Jupyter Python notebook in the Electronic Supplement (**EventDetectSection2.ipynb**). The two RECmin and RECmax parameter sets (Comparison of algorithms for real data, Sect. 3.3 in main text) correspond to the parameter sets sta = 0.03 and lta = 100, sta = 0.54 and lta = 5600, respectively.

	# Total events	# High confidence events (%)	# Low confidence events (%)
All	1856	605 (32.6)	1251 (67.4)
Stick-slip (all)	140	140 (100.0)	0 (0.0)
Teleseismic (all)	68	34 (50.0)	34 (50.0)
Other	1648	472 (28.6)	1176 (71.4)

Table S2. Overview of confidence assignments for known seismicity from the WIS in the multi-sta/LTA catalogue events. High or low confidence is assigned per event in a routine designed to quantify uncertainty of detections. Known seismicity labels for the WIS are only available for stick-slip events (Pratt et al., 2014) and teleseisms from global earthquakes (U.S. Geological Survey, 2022). The 'Other' category is a catch-all container for any events not stick-slip nor teleseismic. Refer to Electronic Supplement for the routine with documentation and corresponding assignments for the reference event catalogue).
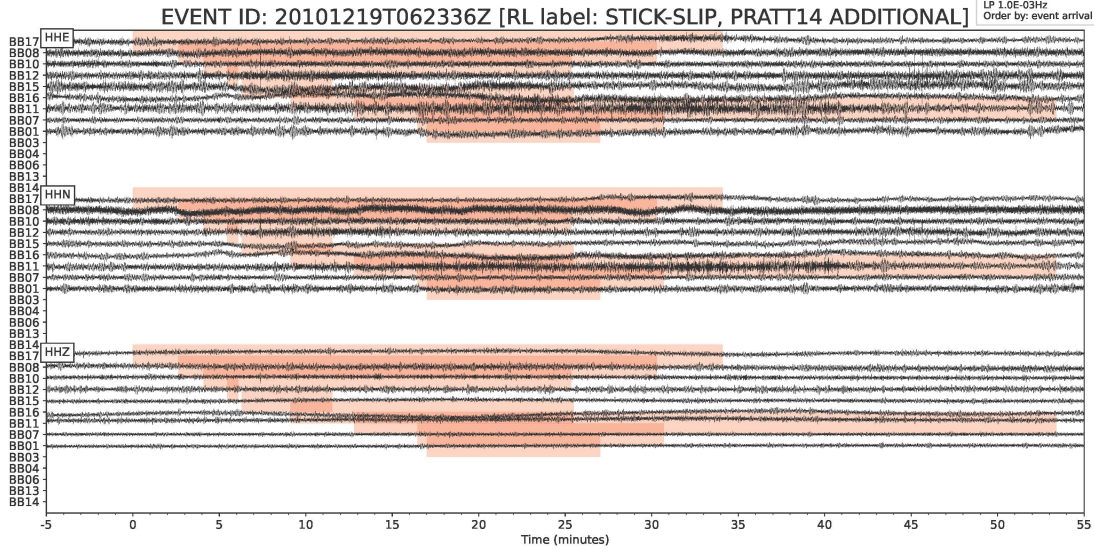
Figure S2. High confidence, stick-slip event from the Whillans Ice Stream 2010–2011 austral summer seismic deployment not previously identified. A bandpass filter has been applied between 0.001 and 1 Hz. Traces are ordered by event arrival time, for the E, N, and Z components. The plotting routine with documentation is provided in Electronic Supplement.

The following supplemental figures are provided to further discussion on the event types identified from the event catalogue compiled with the multi-STA/LTA algorithm. For each event, we show the full seismogram from main text, the network overview, the corresponding spectrogram scaled to the maximum power.
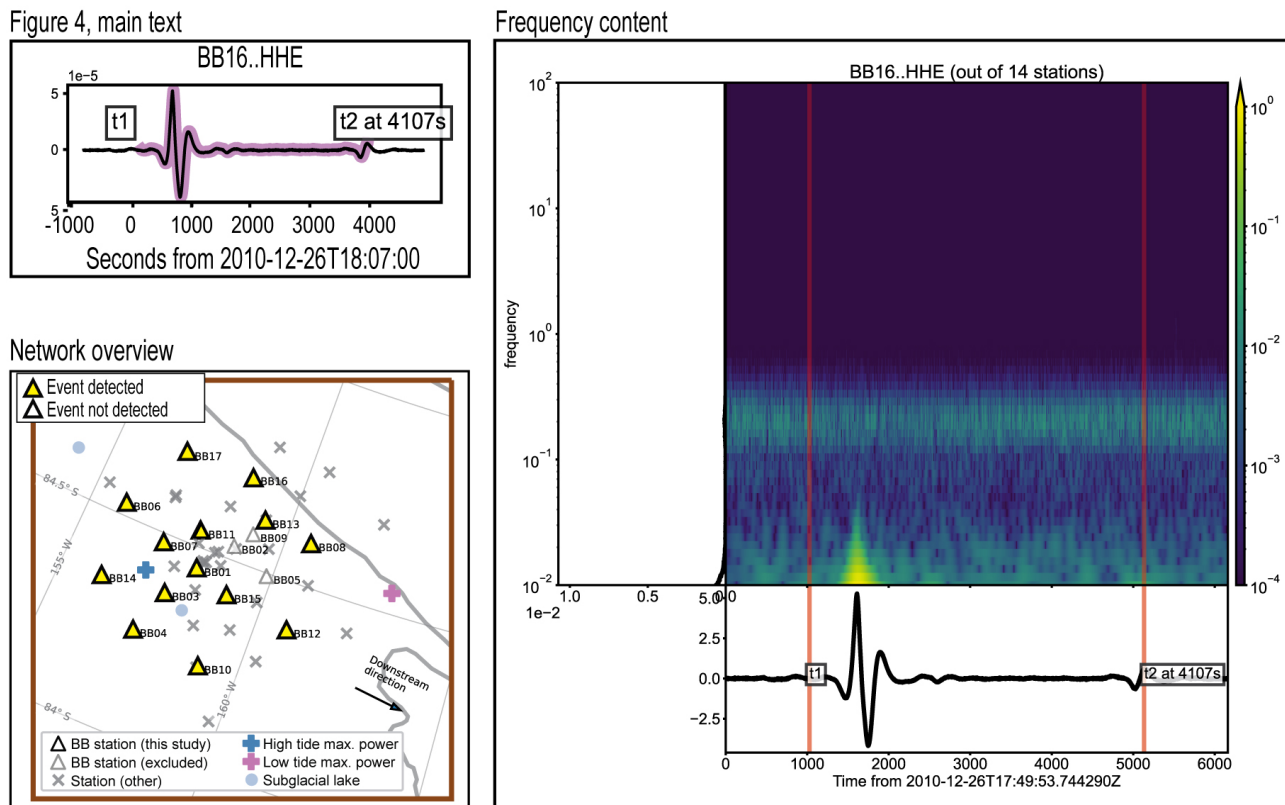
Figure S3. Overview of the stick-slip event type presented in main text. Included is the seismogram of the event shown also in main text, the network overview which shows that all 14 stations detected the event, and the frequency content of the event. The power of the event is constrained at about 10^{-2} Hz, which is expected for stick-slip events (Pratt et al., 2014).
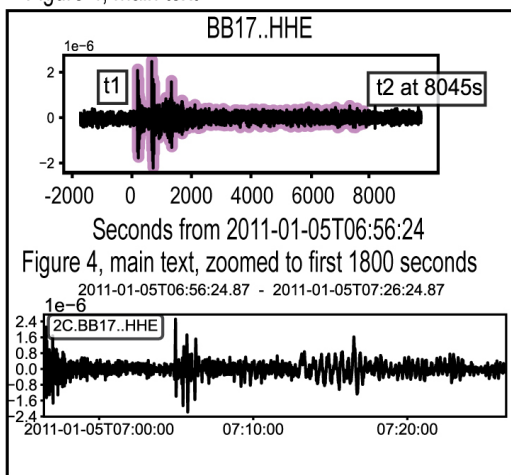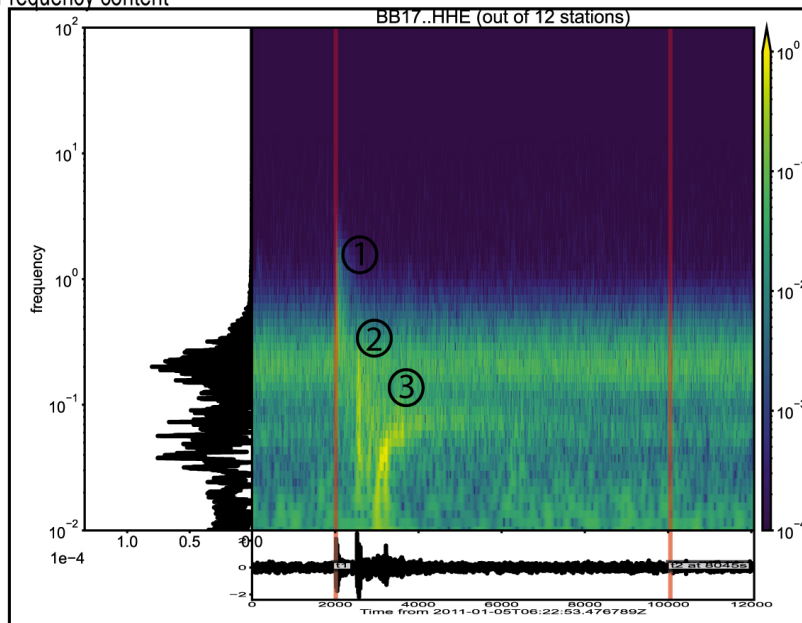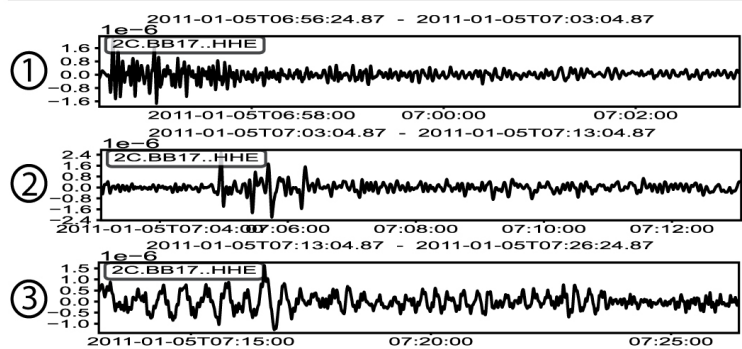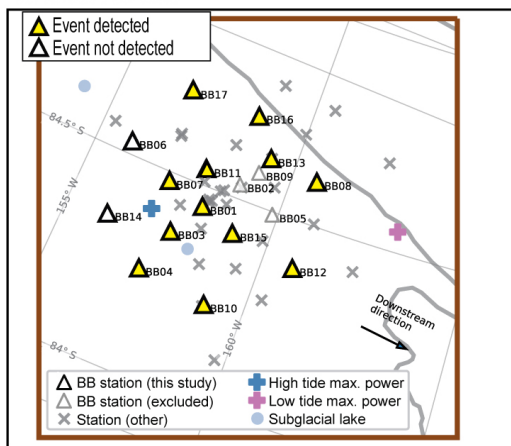
Figure S4. Overview of the Teleseism I event presented in main text. Included is the seismogram of the event shown also in main text and a zoomed in seismogram to the first 1800 seconds, the network overview which highlights the 12 stations that detected the event, and the frequency content of the event. The frequency content falls into three bands, numbered (1), (2), and (3). The seismograms for each of these subsections of the datastream are included below the full spectrogram. The frequency contents for each phase are around (1) 1 Hz, (2) 10^{-1} Hz, and (3) 10^{-2} Hz. The teleseismic source event ruptured 6900 km from the WIS at 2011-01-05T06:46:14 UTC at a depth of 112.2 km (Program, 2011a). The P wave of this earthquake was first recorded near to the WIS ten minutes later, which accounts for the travel time of the earthquake. The event was recorded at Scott Base station at 2011-01-05T06:55:37 UTC, with similar characteristics for first arrival and a high amplitude later arrival (IRIS Wilber 3; Laboratory, 1988). The great circle distances from source to WIS and Scott Base are used to compute travel time, which indicate that the source earthquake should arrive at Scott Base at least 51 seconds before it arrives at WIS. This validates that the event was a true teleseism, as it is shown that the event is detected at Scott Base first by 73 seconds.
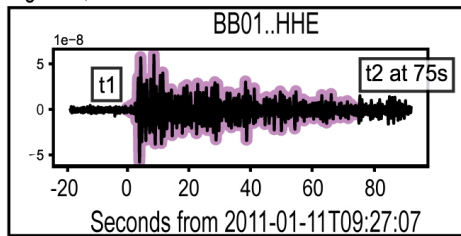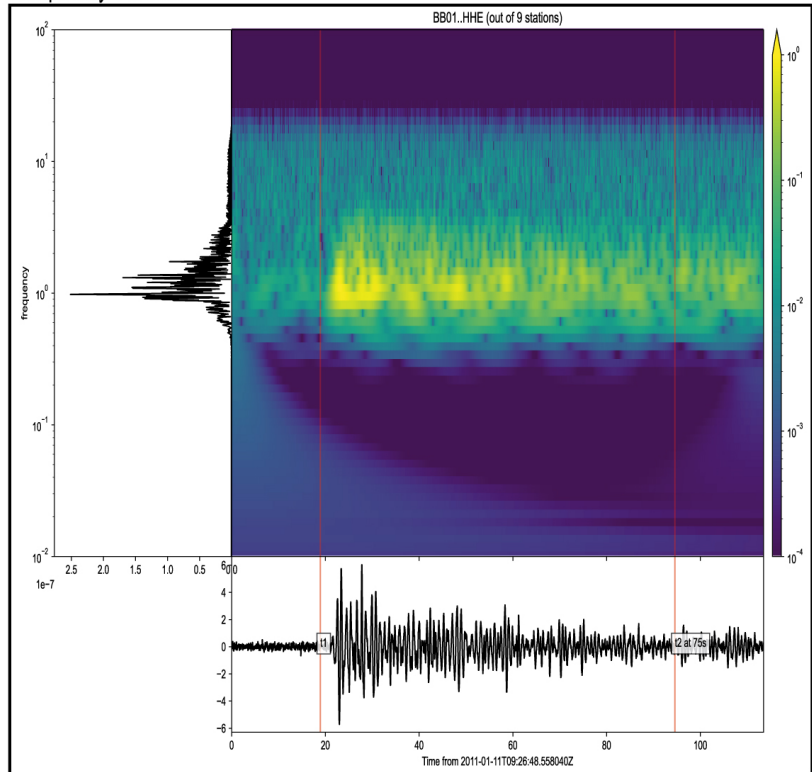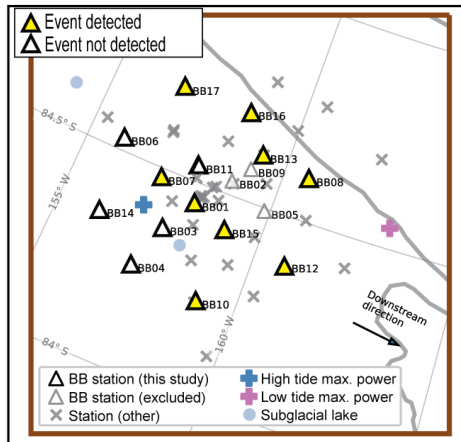
Figure S5. Overview of the Teleseism II event presented in main text. Included is the seismogram of the event shown also in main text, the network overview which shows that 9 stations detected the event, and the frequency content of the event with a bandpass filter applied between 1 and 100 Hz. The teleseismic source event ruptured 8013 km from the WIS at 2011-01-11T09:16:09 UTC at a depth of 221.8 km (Program, 2011b).
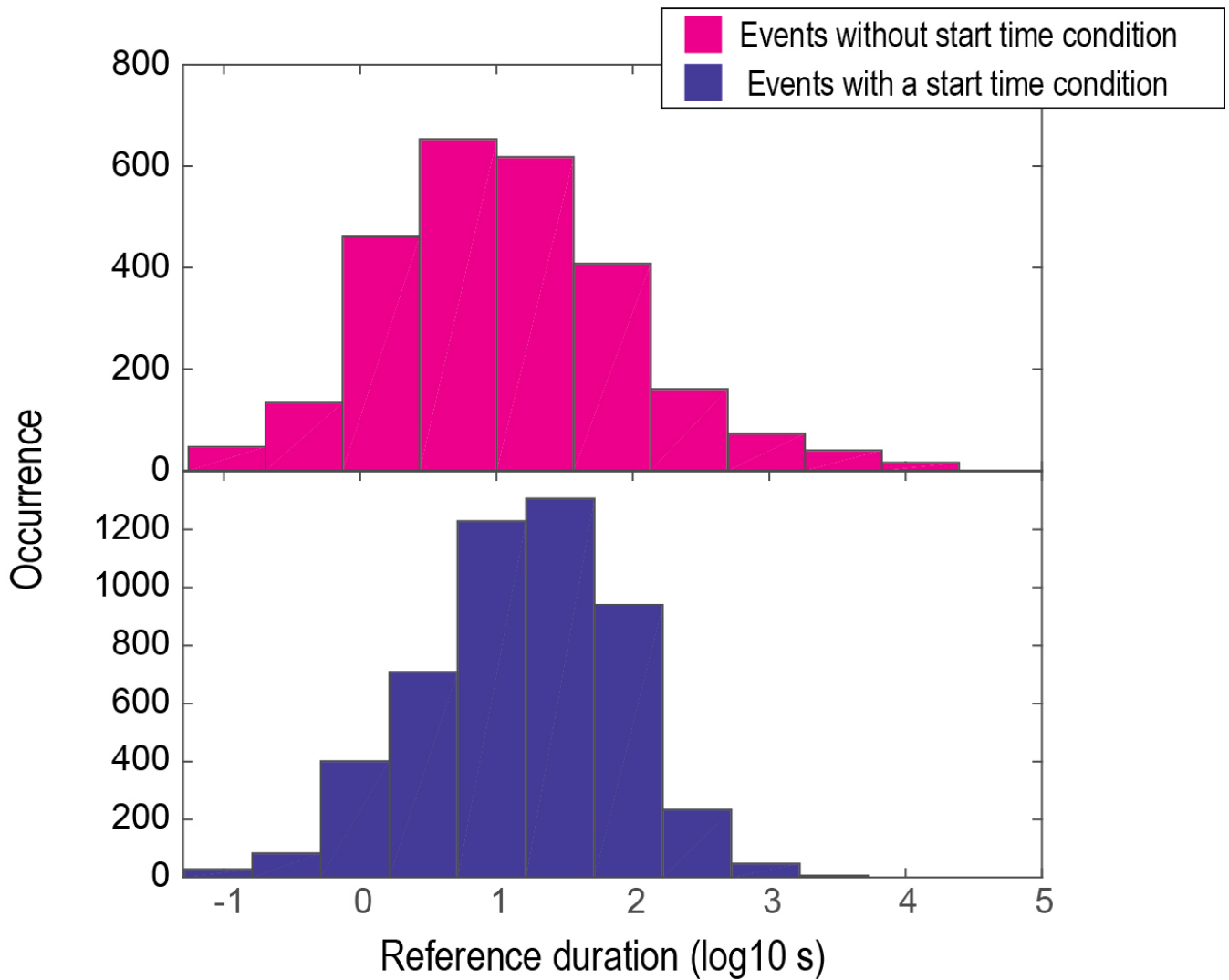
Figure S6. A note on the definitions of an event. Comparison between the reference duration distributions for the event catalogues without and with a start time condition, as discussed in main text. The event catalogue without a start time condition (pink) includes more events with longer durations than the event catalogue with a start time condition (dark blue). This demonstrates the bias towards impulsive initial arrivals for detection with a start time condition. This also demonstrates the ability to detect long, potentially stick-slip type events by detection without a start time condition.